Primary ion fluence dependence in time-of-flight SIMS of a self-assembled monolayer of octadecylphosphonic acid molecules on mica discussion of static limit[1]

M. Nieradko, N.W. Ghonaim, L. Xi, H.Y. Nie, J. Francis, O. Grizzi, K. Yeung, and W.M. Lau

Abstract: By using a self-assembled monolayer of octadecylphosphonic acid molecules, $CH_3(CH_2)_{17}PO(OH)_2$, on mica as a model of the "soft" materials, such as self-assembled monolayers (SAMs) and multilayers in many biological systems as well as artificially engineered molecular electronic systems, we have examined the effects of primary ion fluence on time-of-flight secondary ion mass spectrometry (TOF-SIMS) of the technologically important model. Our measurements clearly show that although the intensity per unit primary ion fluence of most atomic ions and many small fragment ions do not vary by more than 10% for the fluence range of 10^{10}–10^{13} cm^{-2}, the intensity of the parent molecular ion can drop by two orders of magnitude in this fluence range. While the changes are different for the primary ion beams of Bi_3^+ (25 keV, 45°), Bi^+ (25 keV, 45°), and Ar^+ (8 keV, 45°), they are all substantial, with the damage cross section induced by the Bi_3^+ beam being the largest (6 000 $Å^2$). Since different secondary ions have quite different intensity changes, the analytical results derived from TOF-SIMS can vary significantly by the time and duration of the measurements in the TOF-SIMS experiment. Therefore, our results suggest that for TOF-SIMS of molecular layers such as SAMs, the primary ion fluence condition should be recorded and reported. In general, the validity of the static condition becomes questionable when the cumulative primary ion fluence exceeds 1×10^{11} cm^{-2}.

Key words: SIMS, static SIMS, TOF-SIMS, soft materials, self-assembled monolayer, bilayer, surface of biological materials.

Résumé : En prenant une monocouche autoassemblée de molécules d'acide octadécylphosphonique, $CH_3(CH_2)_{17}PO(OH)_2$, sur du mica comme modèle des matériaux souples, tels les monocouches autoassemblées (MAA) et les multicouches qu'on retrouve dans plusieurs systèmes biologiques ainsi que les systèmes électroniques moléculaires mis en place artificiellement, on a examiné les effets de la fluence ionique primaire sur la spectrométrie de masse de l'ion secondaire en temps de vol (SMIS-TDV) du modèle technologiquement important. Nos mesures montrent clairement que, même si l'intensité par unité de fluence de l'ion primaire de la plupart des ions atomiques et que plusieurs petits ions fragments ne varient pas plus de 10% pour la plage de fluence allant de 10^{10} à 10^{13} cm^{-2}, l'intensité de l'ion moléculaire parent peut diminuer par deux ordres de grandeur dans cette plage de fluence. Même si les changements diffèrent avec les divers faisceaux des ions primaires du Bi_3^+ (25 keV, 45°), Bi^+ (25 keV, 45°) et Ar^+ (8 keV, 45°), ils sont toutefois toujours importants et la section droite du dommage induit par le faisceau de Bi_3^+ est le plus important (6 000 $Å^2$). En se basant sur le fait que les changements dans les intensités varient d'une façon importante avec la nature des ions secondaires, les résultats analytiques obtenus à l'aide de la spectrométrie de masse de l'ion secondaire en temps de vol peuvent donc varier d'une façon significative avec le temps et la durée des mesures faites de cette façon. Les résultats obtenus suggèrent donc que pour les SMIS-TDV de couches moléculaires telles que les monocouches autoassemblées, la condition primaire de fluence ionique devrait être enregistrée et rapportée. En général, la validation de la condition statique peut être remise en question quand la fluence cumulative de l'ion primaire dépasse 1×10^{11} cm^{-2}.

Received 14 June 2007. Accepted 24 September 2007. Published on the NRC Research Press Web site at canjchem.nrc.ca on 22 November 2007.

M. Nieradko, N.W. Ghonaim,[2] L. Xi, H.Y. Nie, J. Francis, and W.M. Lau.[3] Surface Science Western, University of Western Ontario, London, ON N6A 5B7, Canada.
K. Yeung.[2] Department of Chemistry, University of Western Ontario, London, ON N6A 5B7, Canada.
O. Grizzi. Centro Atomico Bariloche, CNEA, Instituto Balseiro, UNC & CONICET, Bustillo 9500, 8400 Bariloche, RN, Argentina

[1]This article is part of a Special Issue dedicated to Professor G. Michael Bancroft.
[2]Present address: Department of Biochemistry, University of Western Ontario, London, ON N6A 5B7, Canada.
[3]Corresponding author (e-mail: llau22@uwo.ca).

 doi:10.1139/V07-123 © 2007 NRC Canada

Mots-clés : spectrométrie de masse de l'ion secondaire (SMIS), SMIS statique, spectrométrie de masse de l'ion secondaire en temps de vol (SMIS-TDV), matériaux mous, monocouche autoassemblée, bicouche, surface de matériaux biologiques.

[Traduit par la Rédaction]

Introduction

The surface analytical technique of static secondary ion mass spectrometry (static SIMS), as a means of nondestructive characterization, is now widely used for many surface science applications (1). One emerging field of applications bearing particular importance is the analysis of "soft" molecular layers in both molecular electronics and biological systems, soft materials that include submonolayers of adsorbed organic molecules, self-assembled monolayers (SAM), bi-layer and multi-layer lipid molecules, cell membranes, and surfaces of other biological systems (2–9). They are soft because the intermolecular bonding is commonly van der Waals in nature. In these studies the characterization often requires the detection and imaging of the parent and fragment ions of a constituent with a concentration much less than a monolayer. SIMS, in conjunction with the time-of-flight (TOF) technique, is indispensable because of its rather unique capability in detecting such a trace surface concentration. This detection sensitivity allows the completion of an analysis with a very low primary ion irradiation fluence so that in the course of the analysis only very few of the surface atoms and (or) molecules are struck by a primary ion. As such, when they are probed, all the atoms and (or) molecules are likely in their original condition because all prior probing events are too far away to affect them. Under this "static" condition the SIMS signals can be used to deduce the very original nature of the surface. The accomplishment of this measurement outcome is attractive to most studies, including studies of molecular layers in molecular electronics and biological systems. However, the soft nature of these molecular layers makes them susceptible to changes induced by ion bombardment; hence, further clarification of the static condition in this context is required.

By definition, the maximum primary ion fluence below which the static condition is valid really depends on the radial range of the surface interactions induced by the arrival impact of a specific primary ion on a specific surface. Hence, the static condition itself is by no means "static", and it is more difficult to satisfy when the surface is soft and more susceptible to ion-induced changes. In fact, in the early development of static SIMS most specimens of interest were stable inorganic materials with surfaces relatively immune to ion-induced changes. The radial range is often correlated to the collision cross-section, which is typically about 10^{-14} cm^2 for most ion bombardment at the keV range for many metals, semiconductors, and dielectrics (10–12). For an analysis of this type, the static condition can be quite forgiving and is often specified with a primary ion fluence lower than 1×10^{13} cm^{-2}. In 1991 and 1992, Legett and Vickerman measured (13–14) the primary ion fluence dependence of secondary ion signals from polymers poly(ethylene terephthalate), poly(tetrafluoroethylene), poly(vinyl chloride), and poly(methyl methacrylate) and showed the damage of the original nature of the polymer caused by both ion bombardment and ion neutralization. In 1995, Delcorte et al. (15) cautioned any casual claim of nondestructive measurements and insightfully proclaimed that there is no real "static" condition, and one should always be careful about bombardment-induced effects during any ion beam analysis. In 1996, Gilmore and Seah (16) carefully examined the static SIMS condition for polymers such as poly(ethyleneterephthalate) and poly(tetrafluoroethylene) with 4 keV argon and xenon primary ions and made the practical recommendation that for the analysis of polymers, the primary ion fluence limit for maintaining the static condition should not be higher than 1×10^{12} cm^{-2}. Since then, most studies of soft materials have indeed adopted this recommendation.

Because primary ion bombardment effects on soft molecular layers have not yet been studied thoroughly, we have begun to study the effects of primary ion fluence in TOF-SIMS and TOF ion scattering spectroscopy (ISS) for the soft molecular layers in the molecular electronics and biological systems in our own on-going research. In this article, we report on some of our results collected from the special specimens of octadecylphosphonic acid, $CH_3(CH_2)_{17}PO(OH)_2$, on mica in the form of a self-assembled monolayer (referred to as OPA/mica, with the molecule referred to as OPA-H). These specimens were used to model the silane-based and phosphyl-based molecular layers in molecular electronics and cell membranes. They were also chosen because our research group had already acquired some prior knowledge on their formation mechanism and technical skills on the use of TOF-SIMS and atomic force microscopy (17, 18).

The article will focus on the exemplification of the sensitive TOF-SIMS changes in the fluence regimes of 10^{11} to 10^{13} cm^{-2}, with some data points collected below 10^{11} cm^{-2} whenever the data collection is practical. Since the Bi_3^+ ion beam is one of the primary ion beams of choice in the recent research of soft molecular layers, most of the results shown in this article were collected with it. To illustrate some of our ideas on the possible ion–surface interactions causing the observed sensitivity of primary ion fluence, we will also show some TOF-SIMS results of Bi^+ and Ar^+ on OPA/mica and of Bi_3^+ on alkyl-thiols/Au(111).[4] In addition, we will briefly correlate these results with those from our scanning probe microscopic studies of the ion–surface interactions on these molecular layers (19).

Results and discussion

Primary ion fluence dependence of negative secondary ions from OPA/mica with Bi_3^+

As expected, the secondary parent ion intensity critically depends on the primary ion fluence for the model molecular layer sample of OPA/mica in the entire primary ion fluence

[4] N. Ghonaim. Manuscript in preparation.

© 2007 NRC Canada

Fig. 1. Relative TOF-SIMS negative secondary ion intensities as a function of primary ion fluence for OPA on mica using a Bi_3^+ ion beam within a cumulative primary ion fluence of (*a*) 10^{13} cm^{-2} and (*b*) 10^{12} cm^{-2}.

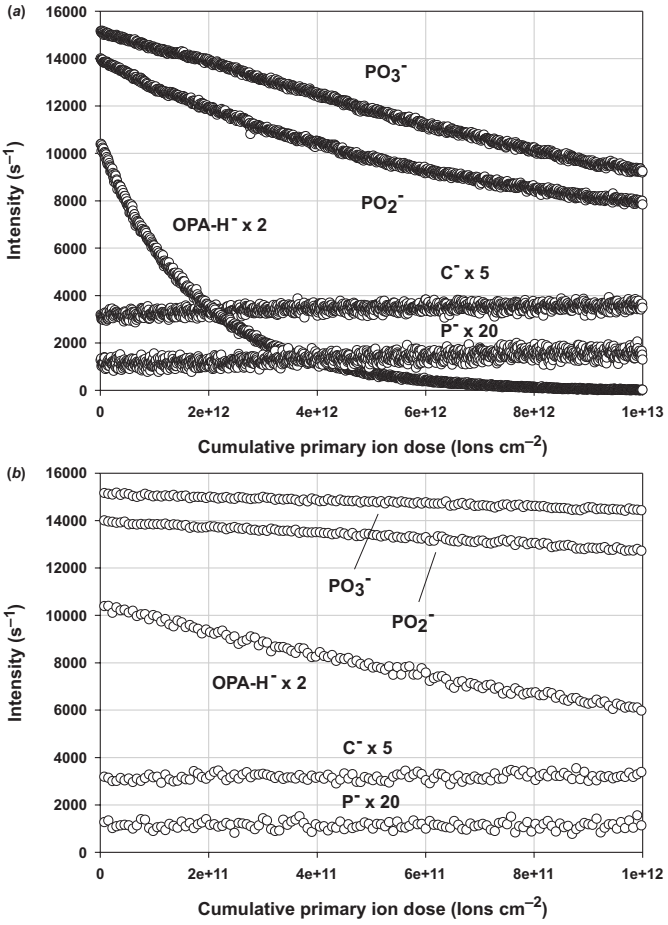

range from about 1×10^{10} to 1×10^{13} cm^{-2}. Negative secondary ion intensities are shown in this example because the negative secondary ion yield is much higher than the positive ion counterpart. The comparison between negative and positive secondary ions can be found later in the paper. From Figs. 1*a* and 1*b*, one sees that the parent molecular ion (OPA-H$^-$) drops exponentially, with a decrease in intensity of two orders of magnitude when the cumulative primary ion fluence increases from 1×10^{10} to 1×10^{13} cm^{-2}. Similarly, the characteristic phosphate fragments PO_3^- and PO_2^- decrease in intensity immediately as well, but these changes are much less marked within 1×10^{12} cm^{-2}. The measured changes are definitely not caused by any system error because the negative fragment ion intensity of elemental carbon (C$^-$) and phosphorus (P$^-$) change very little in the same cumulative primary ion fluence range. Conceivably the bombardment leads to bond breakage in the adsorbed molecules causing a drop in the concentration of the virgin molecules. The bond breakage, on the other hand, increases the number of carbon atoms having dangling bonds, which may lead to the observed increase in the C$^-$ intensity. As revealed in the following sections, the C$^-$ intensity for TOF-SIMS with Bi^+ and Ar^+ and that of C^+ for Bi_3^+ also increase with increasing cumulative primary ion fluence. All these observations, together with the observations that the parent ion intensities in all these bombardment conditions consistently decrease exponentially with the cumulative primary ion fluence, converge to the inference that the primary ion bombardments in all these cases are causing a very significant damage to the adsorbed molecules. To further support the results shown by the plots of the primary ion fluence dependence of the selective ions in Fig. 1, we show the negative ion mass spectra of OPA/mica at a cumulative primary ion fluence of 1×10^{11} cm^{-2} (Fig. 2*a*) and 1×10^{13} cm^{-2} (Fig. 2*b*) and those of a bare mica at a cumulative primary ion fluence of 1×10^{13} cm^{-2} (Fig. 2*c*). Once again, the parent molecular ion intensity in Fig. 2*a* drops rapidly in Fig. 2*b* and is obviously absent in Fig. 2*c*. In Fig. 2*b*, some fragments derived from the bombardment damage of OPA, such as PO_2^- and PO_3^-, are seen; once again, they are absent in Fig. 2*c*. A comparison of Figs. 2*a* and 2*b* also shows that the intensity drop for the OPA parent molecular ion is much more significant than those of the PO_2^- and PO_3^- fragment ions. While no signals from the mica substrate are seen in Fig. 2*a*, they appear in Fig. 2*b*. However, this does not necessarily mean that a large fraction of the OPA coverage has been completely removed, because the PO_2^- and PO_3^- signals are still strong in Fig. 2*b* and a careful examination of the intensity of P$^-$ (see also Fig. 1*b*) shows little change up to a primary ion fluence of 1×10^{13} cm^{-2}.

In principle, the observed exponential decrease of the parent molecular secondary ion intensity is a convoluted effect of damage and removal of the OPA molecule, together with the possible change in ion yield. However, OPA removal due to sputtering or desorption should not be an important attribute in the low primary ion fluence range of the present work. For example, if a removal yield of 10 molecules per primary ion is assumed, the decrease in OPA surface density should still be less than 10% for a primary ion fluence of 1×10^{13} cm^{-2}. There are further experimental observations supporting the insignificance of OPA removal. First, the P$^-$ intensity does not change significantly at the primary ion fluence of 1×10^{13} cm^{-2}, as shown in Fig. 1. If removal of OPA is important, one would expect a significant drop in the P$^-$ intensity. Second, an atomic force microscopic analysis of the sample after receiving a primary ion fluence of 1×10^{13} cm^{-2} shows no void in the self-assembled monolayer. Regarding the ion yield factor, subsequent sections of this article show that similar exponential decreases of the parent molecular ion intensity are evident for positive ion measurements with Bi_3^+ and negative ion measurements with Ar^+ and Bi^+. This indicates that the observed exponential decreases of the parent molecular ion intensity in all these cases are mainly due to the damage of the parent molecules induced by the primary ion bombardment.

To further analyze the observed secondary parent ion intensity changes as a function of primary ion fluence, we assume that the observed exponential drop of the parent molecular ions is due to the damage of the parent molecule, OPA-H, by the primary ion bombardment. Taking this assumption, we adopt the following common description with the concept of damage cross-section (1),

$$[1] \qquad I_t(\phi) = I_o \exp(-\sigma\phi)$$

where I_o and I_t are the respective secondary parent ion intensities at the beginning of the measurements and at time t, ϕ is

© 2007 NRC Canada

Fig. 2. TOF-SIMS negative secondary ion mass spectra for OPA on mica using a Bi_3^+ ion beam within a cumulative primary ion fluence of (*a*) 1×10^{11} cm^{-2} and (*b*) 1×10^{13} cm^{-2}. The spectrum from bare mica with a cumulative primary ion fluence of 1×10^{13} cm^{-2} is included in (*c*).

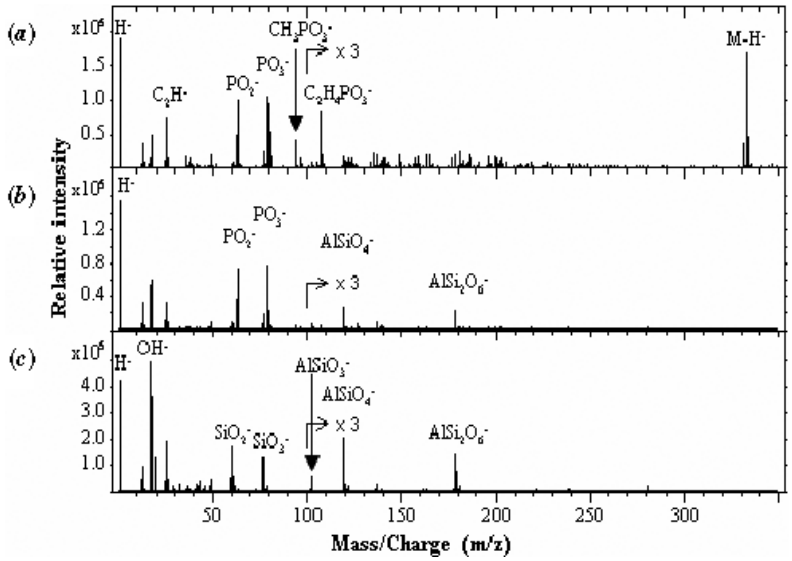

the cumulative primary ion fluence after time *t*, and σ is the damage cross-section for the parent molecule. It turns out that the damage cross-section of the parent OPA-H$^-$ molecule by Bi_3^+ at 25 keV and at an incident angle of 45° is about 6×10^{-13} cm^2 (or 6 000 Å^2). This is consistent with the work by Galera et al. (20) on the Langmuir–Blodgett monolayer of arachidic acid on gold with 2 keV Cs^+ and an ion incident angle of 20°. The damage cross-section in this previous case is ~1×10^{-13} cm^2. In comparison, Benninghoven and Sichtermann (11) reported significantly smaller damage cross-sections (from 1 to 7×10^{-14} cm^2) for various parentlike ions from a sample of leucine (with 2.25 keV Ar^+ as the primary ion). We speculate that the relative large damage cross-sections for molecular layers such as self-assembled monolayers and Langmuir–Blodgett films may arise from the agility of the damaged molecules and their diffusion inevitably extends the radial range of molecular damage.

With the estimated damage cross-section value of 6×10^{-13} cm^2 and eq. [1], we can further calculate the primary ion fluence limit for the static condition by adopting the Gilmore and Seah recommendation of setting the fluence limit by allowing not more than a 10% change in the secondary ion intensity. The result in this case is 2×10^{11} cm^{-2}, which is significantly lower than the prevalent assumption of a fluence limit of 1×10^{12} cm^{-2} for the static condition. If this prevalent fluence limit assumption were adopted in the study of OPA/mica under the same analysis condition in this work, the maximum secondary ion intensity change in the fluence range of 1×10^{12} cm^{-2} is 39%. Obviously, the claim of the static condition is invalid.

What are the practical scientific implications of erroneously going beyond the primary ion fluence limit of the static condition? The immediate implication is that any measurements of the surface density of a molecule with a large damage cross-section will become rather arbitrary when the measurements only claim the validity of the static condition without specifying the actual cumulative primary ion fluence for the measurements. In addition, rectifying this error by resorting to calculations of relative intensities with one molecular species as an internal reference may not work because the damage cross-sections are likely molecule and (or) fragment dependent, even for the same primary ion bombardment conditions. For example, the data in Fig. 1 clearly show that the damage cross-section for OPA-H$^-$ is higher than PO_3^- and PO_2^-. Hence, we advocate that in TOF-SIMS studies of soft molecular layers, one should mind the effects of primary ion fluence. With our estimated primary ion fluence limit of 2×10^{11} cm^{-2} for OPA/mica with 25 keV Bi_3^+, we recommend that the static condition should be set to 1×10^{11} cm^{-2} for TOF-SIMS studies of soft molecular layers. However, we prefer to recommend that a thorough check of the primary ion fluence dependence is the best remedy for reducing any measurement errors induced by the dependence of primary ion fluence.

Primary ion fluence dependence of positive secondary ions from OPA/mica with Bi_3^+

Under Bi_3^+ bombardment, the detection of negative secondary ions commonly gives more intense signals than that of positive secondary ions from an oxide matrix. For the sake of completeness of illustrating the primary ion fluence dependence in this work, we show the secondary ion intensities of OPA+H$^+$ and C$^+$ as a function of primary ion fluence in Figs. 3*a* and 3*b*. Although the signal-to-noise statistics displayed in Fig. 3 are far from ideal, the data do show clearly that while the intensity of C$^+$ increases slowly, the parent molecular ion intensity drops rapidly. When we fit the data for OPA+H$^+$ using eq. [1], we obtain a damage cross-section of ~ 5×10^{-13} cm^{-2}. Because the signal-to-noise level of this set of data is poor, we do not speculate on any difference in damage cross-section or damage mechanism between the negative secondary ion detection and the positive ion detection.

© 2007 NRC Canada

Fig. 3. Relative TOF-SIMS positive secondary ion intensities as a function of primary ion fluence for OPA on mica using a Bi_3^+ ion beam within a cumulative primary ion fluence of (*a*) 10^{13} cm^{-2} and (*b*) 10^{12} cm^{-2}.

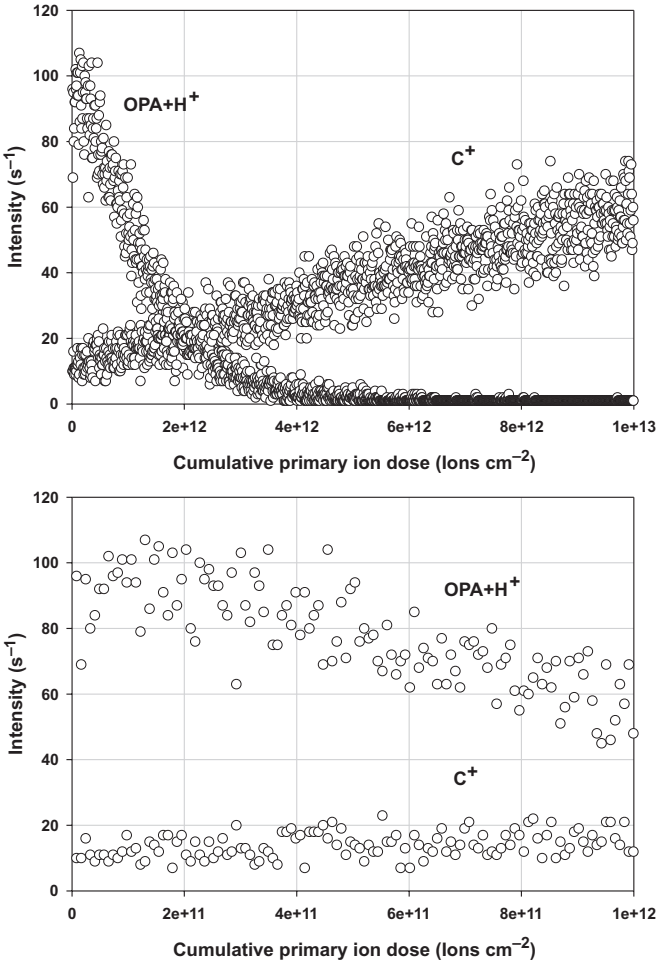

Fig. 4. Relative TOF-SIMS negative secondary ion intensities as a function of primary ion fluence for OPA on mica using a Bi^+ ion beam within a cumulative primary ion fluence of (*a*) 10^{13} cm^{-2} and (*b*) 10^{12} cm^{-2}.

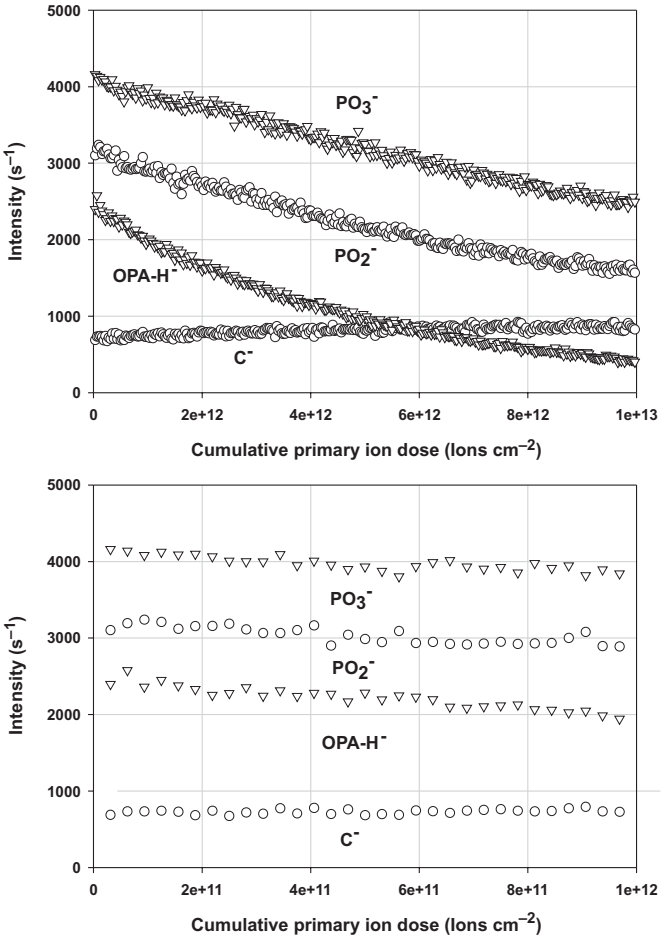

Comparison of the results from OPA/mica with Bi_3^+ with those with Bi^+ and Ar^+

Our preliminary results from bombardment of the OPA/mica by a 25 keV Bi^+ source shows similar dependencies on primary ion fluence for OPA-H$^-$ and C$^-$ as well as the characteristic phosphate headgroups PO_3^- and PO_2^-, as shown in Figs. 4*a* and 4*b*. The intensity of the carbon fragment ion slowly increases throughout the experiment while the intensity of the parent molecular ion drops exponentially. As expected, the Bi_3^+ ion beam outperforms the Bi^+ ion beam in producing characteristic secondary ion intensities in the same fluence range because of the nature of cluster ion bombardment (2). Fitting of the Bi^+ OPA-H$^-$ profile with eq. [1] gives a damage cross-section of 2×10^{-13} cm^2. For comparison purposes, bombardment of the OPA/mica by an 8 keV Ar^+ source is shown in Figs. 5*a* and 5*b*. The molecular ion is only weakly detected compared with using either of the bismuth ion sources. As a result, each point of the profile is summed over five scans to give a less noisy appearance. Fitting of the Ar^+ OPA-H$^-$ profile with eq. [1] gives a damage cross-section of 3×10^{-13} cm^2. The smaller damage cross-section of OPA-H$^-$ using the Bi^+ source compared with the Bi_3^+ source is expected, as discussed in the literature with various studies of thin organic layers under cluster ion bombardment (3, 5). The kinetic energy of the Bi^+ source is 25 keV while that of the Bi_3^+ source is ~8 keV per atom. Therefore the Bi^+ source will penetrate deeper into the specimen while producing less damage in the near-surface plane compared with each atom of the Bi_3^+ source.

With the readily available TRIM/SRIM codes for studying molecular dynamics in the collision cascades, we use a hypothetical sample of 2 nm polyethylene on alumina to cross-check the effects of primary ion bombardment for Bi^+ (25 keV, 45°), Bi^+(8 keV, 45°), and Ar^+ (8 keV, 45°). The calculations give the 3-dimensional ion, recoil, and vacancy distribution statistics, and have been prevalently used in the interpretation of SIMS results (2, 5). In the present work, we find that Ar^+ at 8 keV produces 3 to 4 carbon vacancies and 10 hydrogen vacancies per Ar^+ in the polymer layer, which is about two times less than Bi^+ at 25 keV. However, the lateral range of the vacancy distribution in the polymer layer in both cases is about the same. This may be the reason the damage cross-section of Ar^+ at 8 keV is close to that of Bi^+ at 25 keV. Although the TRIM calculations do not take into

© 2007 NRC Canada

Fig. 5. Relative TOF-SIMS negative secondary ion intensities as a function of primary ion fluence for OPA on mica using an Ar^+ ion beam within a cumulative primary ion fluence of (*a*) 10^{13} cm^{-2} and (*b*) 10^{12} cm^{-2}.

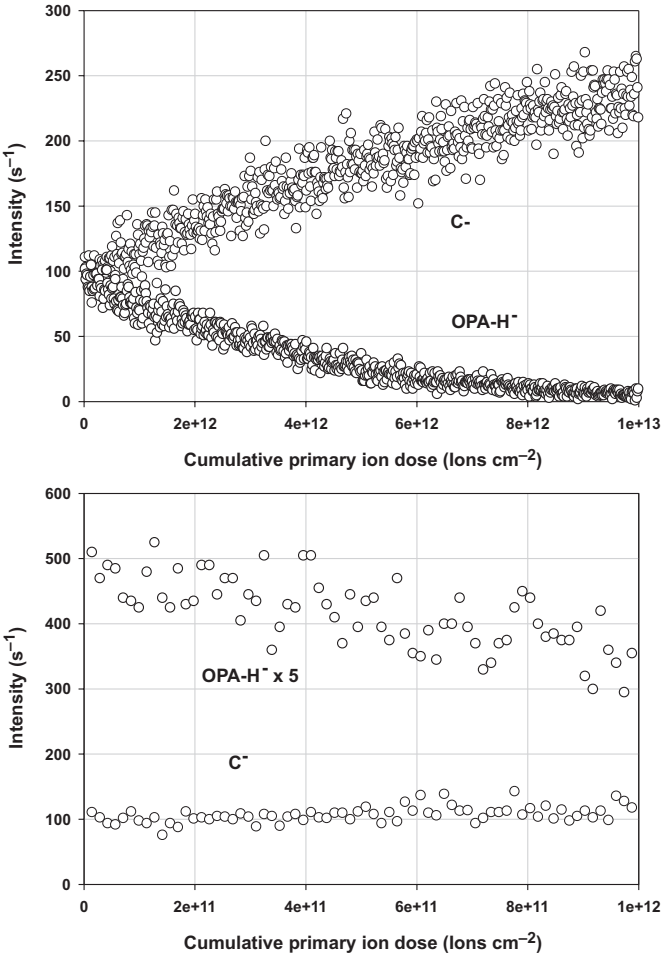

account many-body interactions and likely over-simplify the collision cascade activities induced by cluster ion bombardment, we find that three Bi^+ ions at 8 keV produce at least two times more hydrogen and carbon vacancies in the top polymer layer than 1 Bi^+ at 25 keV. Our experimental results show that the damage cross-section of Bi_3^+ at 25 keV is indeed larger than that of Bi^+ at 25 keV.

Comparison of the SIMS results from OPA/mica with those from alkyl-thiols/Au(111)

In our on-going research on TOF-SIMS and TOF-ISS of soft molecular layers, we have used the OPA/mica model to represent the silane and phosphyl self-assembled monolayer families and the alkyl-thiol/Au(111) model to represent the thiol self-assembled monolayer family. Briefly, the TOF-SIMS of the alkyl-thiol/Au(111) model is also sensitively dependent on the primary ion fluence, and the primary ion fluence limit for the static condition is also much lower than 1×10^{12} cm^{-2}. Hence, the extent of molecular damage is not fundamentally different from the OPA/mica model. In fact, our TOF-ISS studies of the alkyl-thiol/Au(111) model, which detect neutral recoil emission as well as ion emission from the surface, have also independently confirmed that primary ion fluence causing damage to 10% of surface molecules is below 1×10^{12} cm^{-2}, even for 4 keV Ar^+ (20° incidence).[5] Although the TOF-SIMS of the OPA/mica and the alkyl-thiol/Au(111) model are both influenced by molecular damage, the overall primary ion fluence dependence of the alkyl-thiol/Au(111) model is different from that of the OPA/mica model. For example, while the SIMS signals of the large molecular ions from OPA/mica generally drop exponentially, those from thiols/Au do not change monotonically. In other words, those from thiols/Au are quite complicated. The difference arises from the fact that during TOF-SIMS with a reactive primary ion such as bismuth, cesium, or oxygen, the primary ion bombardment does not only cause molecular damage but also affects the relative ion yields of some ions. By examining the intensity changes of all secondary ions (or the lack of changes) in the OPA/mica model with Bi_3^+ (both negative secondary ions and positive secondary ions), Bi^+ (negative secondary ions), and Ar^+ (negative secondary ions), we have not observed any obvious ion yield changes induced by the accumulation of primary ion fluence. In comparison, the ion yield changes are very obvious in the alkyl-thiols/Au model. The detailed description of the results collected from the alkyl-thiol/Au(111) model will be given elsewhere.[4]

Complementary results from scanning probe microscopy of relevant model specimens

In the present study of the OPA/mica model, we have used atomic force microscopy to verify the presence of a "complete" monolayer of OPA molecules on a freshly cleaved flat mica surface. In this context, complete means no observation of any detectable voids in the layer. After the TOF-SIMS experiments, we used AFM to track the molecular damage inferred from the TOF-SIMS data. Interestingly, no clear evidence of void formation has been detected. The fact that the molecular damage inferred from TOF-SIMS is not accompanied by sputter removal or desorption of the molecules is further confirmed by the observation of a constant P^- intensity for a primary ion fluence up to 1×10^{13} cm^{-2} in the Bi_3^+ experiment, which has the highest damage cross-section. As mentioned earlier in this article, we speculate that the "molecular damage" inferred from the changes of parent molecular ion intensity may be the combined effect of the fragmentation of some parent molecules being influenced by a primary ion arrival and the diffusion of the altered molecules. Drastic removal of the parent or altered molecules from the surface are not necessary conditions for the observed primary ion fluence dependence of secondary ion intensity. If so, AFM cannot detect the surface chemistry changes induced by the primary ion fluence.

We want to note in this discussion that in our recent examination of short-chain alkyl-thiols on Au(111), we have observed from scanning tunneling microscopy that while the original surface lattice of short-chain alkyl-thiols (C_2H_5S or C_3H_7S) on Au(111) is ordered, a seemingly armless ion bombardment with a low fluence of 10 eV H^+ can cause some drastic changes on the ordering of the surface lattice

[5] O. Grizzi. Manuscript in preparation.

© 2007 NRC Canada

and clear evidence of bombardment-induced diffusion of molecules can be recorded (19). This set of new results supports our speculation of a "fragmentation + diffusion" mechanism causing our observed sensitive primary ion fluence on TOF-SIMS analysis of a soft molecular layer.

Conclusion

The primary ion fluence effects on the TOF-SIMS data from an octadecylphosphonic acid (OPA) self-assembled monolayer (SAM) on freshly cleaved mica (muscovite) have been studied with Bi_3^+, Bi^+, and Ar^+ primary ion beams. The parent molecular secondary ions in all change rather drastically as a function of primary fluence below 1×10^{11} to 1×10^{13} cm^{-2}. Fitting of the OPA-H^- data (Bi_3^+ ion beam, 25 keV, 45° incident angle) to a single exponential function gives a damage cross-section of 6×10^{-13} cm^2 (6 000 $Å^2$) for the parent molecular ion. A similar damage cross-section of the parent molecular ion is observed during the collection of positive secondary ions. The static limit for TOF-SIMS of OPA/mica with Bi_3^+ is estimated to be 2×10^{11} cm^{-2}, which is significantly lower than the prevalent static limit of 1×10^{12} cm^{-2} in TOF-SIMS. In comparison to Bi_3^+ (25 keV, 45°), Bi^+ (25 keV, 45°), and Ar^+ (8 keV, 45°) have OPA-H^- damage cross sections of 2×10^{-13} cm^2 and 3×10^{-13} cm^2, respectively. With these data, we recommend that it is safer to set the static condition to 1×10^{11} cm^{-2} for TOF-SIMS of soft molecular layers. Ideally, the primary ion fluence condition and the secondary ion changes as a function of primary ion fluence should be measured and reported.

Experimental

Sample preparation

Crystalline octadecylphosphonic acid (OPA), $CH_3(CH_2)_{17}PO(OH)_2$, was obtained from Alfa Aesar (Ward Hill, Massachusetts). The sample preparation was performed according to the procedure of Nie et al. (16). An OPA SAM of approximately 100% coverage was prepared by spin-coating a 2 mmol/L solution of OPA in trichloroethylene onto freshly cleaved muscovite mica at 5 000 rpm. This coating was then dried with nitrogen to remove any weakly adsorbed molecules or other loose contaminants. The mica was 1 cm x 1 cm in size. Four regions were etched onto this coated mica, one for each TOF-SIMS time profile performed. A second bare piece of muscovite mica was also cleaved for comparison purposes in the TOF-SIMS studies.

AFM measurements

Topography measurements were performed using a PSIA XE-100 microscope. The sample surface was scanned in noncontact, low-voltage mode with a scan area of 1 μm × 1 μm. The low voltage mode was used to observe fine surface features that were present in SAMs

TOF-SIMS measurements

An ION-TOF (Gmbh) TOF-SIMS IV single-stage reflectron instrument with 10 kV post acceleration was used to study the OPA SAMs prepared on the mica substrate. A pulsed, low-energy electron flood gun was used to neutralize sample charging. All measurements were performed at room temperature. The raw data was analyzed using the IonSpec program. All intensities were normalized against the total intensity of each particular spectrum. The lack of detectable damage arising from the low energy electron irradiation during the measurements was confirmed by the fact that no change was observed after the TOF-SIMS measurement was paused, by blanking the primary ion beam without stopping the low energy electron irradiation.

Negative secondary ion OPA on mica time profile with Bi_3^+ source

Negative secondary ion measurements were performed using a (10 kHz) pulsed 25 keV Bi_3^+ primary ion beam at an incidence angle of 45°. The primary ion beam with a pulsed current of 0.12 pA was focused and rastered onto a 128 × 128 μm^2 area, delivering a cumulative ion dose of 1 x 10^{13} ions cm^{-2}.

Negative secondary ion OPA on mica time profile with Bi^+ source

Negative secondary ion measurements were performed using a (10 kHz) pulsed 25 keV Bi^+ primary ion beam at an incidence angle of 45°. The primary ion beam with a pulsed current of 0.5 pA was focused and rastered onto a 128 × 128 μm^2 area, delivering a cumulative ion dose of 1×10^{13} ions cm^{-2}.

Positive secondary ion OPA on mica time profile with Bi_3^+ source

Positive secondary ion measurements were performed under these same conditions and an identical cumulative ion dose. The primary ion beam pulsed current was 0.13 pA.

Positive secondary ion mica time profile with Bi_3^+ source

Positive secondary ion measurements were performed under these same conditions and an identical cumulative ion dose. The primary ion beam pulsed current was 0.13 pA

Negative secondary ion OPA on mica time profile with Ar^+ source

Negative secondary ion measurements were performed using a (10 kHz) pulsed 8 keV Ar^+ primary ion beam at an incidence angle of 45°. The primary ion beam with a pulsed current of 0.182 pA was focused and rastered onto a 256 × 256 μm^2 area, delivering a cumulative ion dose of 1×10^{13} ions cm^{-2}.

Acknowledgement

This work was partially supported by the Natural Sciences and Engineering Research Council of Canada (NSERC) Discovery Grant (Grant No. 327221 06), the NSERC CIAM Grant, Surface Science Western (SSW), and the Faculty of Science of the University of Western Ontario. SSW was founded in 1981 at the University of Western Ontario by several visionary leaders including Professor Mike Bancroft who was its founding director. All authors are grateful to Professor Bancroft for his initiation of the research center and his scientific advice for SSW from 1981 to the present.

© 2007 NRC Canada

References

1. J.C. Vickerman and D. Briggs. TOF-SIMS: Surface analysis by mass spectrometry. IM Publications, Chichester, UK. 2001.
2. S.C.C. Wong, N.P. Lockyer, and J.C. Vickerman. Surf. Interface Anal. **37**, 721 (2005).
3. Y.-P. Kim, M.-Y. Hong, J.M. Kim, E.K. Oh, H. Kyong-Shon, D.W. Moon, H.-S. Kim, and T.G. Lee. Anal. Chem. **79**, 1377 (2007).
4. P.L. Clode, R.A. Stern, and A.T. Marshall. Microsc. Res. Tech. **70**, 220 (2007).
5. D. Debois, A. Brunelle, and O. Laprévote. Int. J. Mass Spectrom. **260**, 115 (2007).
6. Z. Pernber, K. Richter, J.-E. Mansson, and H. Nygren. Biochim. Biophys. Acta, **1771**, 202 (2007).
7. L.G. Wu, X.C. Lu, K.S. Kulp, M.G. Knize, E.S.F. Berman, E.J. Nelson, J.S. Felton, and K.J.J. Wu. Int. J. Mass Spectrom. **260**, 137 (2007).
8. K. Börner, P. Malmberg, J.-E. Månsson, and H. Nygren. Int. J. Mass Spectrom. **260**, 128 (2007).
9. A.M. Piwowar and J.A. Garrdella, Jr. Anal. Chem. **79**, 4126 (2007).
10. A. Benninghoven, D. Jaspers, and W. Sichtermann. Appl. Phys. **11**, 35 (1976).
11. A. Benninghoven and W. Sichtermann. Int. J. Mass Spectrom. Ion Phys. **40**, 177 (1981).
12. W. Lange, M. Jirikowsky, and A. Benninghoven. Surf. Sci. **136**, 419 (1984).
13. G.J. Leggett and J.C. Vickerman. Anal. Chem. **63**, 561 (1991).
14. G.J. Leggett and J.C. Vickerman. Appl. Surf. Sci. **55**, 105 (1992).
15. A. Delcorte, L.T. Weng, and P. Bertrand. Nucl. Instrum. Methods Phys. Res. B, **100**, 213 (1995).
16. I.S. Gilmore and M.P. Seah. Surf. Interface Anal. **24**, 746 (1996).
17. J.T. Francis, H.-Y. Nie, N.S. McIntyre, and D. Briggs. Langmuir, **22**, 9244 (2006).
18. H.-Y. Nie, M.J. Walzak, and N.S. McIntyre. J. Phys. Chem. B, **110**, 21101 (2006).
19. L. Xi, W.M. Lau, and O. Grizzi. Appl. Surf. Sci. In press.
20. R. Galera, J. Blais, and G. Bolbach. Int. J. Mass Spectrom. Ion Proc. **107**, 531 (1991).

© 2007 NRC Canada